Science in China Series A: *Mathematics*
Aug., 2008, Vol. 51, No. 8, 1510–1521
www.scichina.com math.scichina.com
www.springerlink.com

A moving boundary problem derived from heat and water transfer processes in frozen and thawed soils and its numerical simulation

XIE ZhengHui[1†], SONG LiYe[1,2] & FENG XiaoBing[3]

[1] Institute of Atmospheric Physics, Chinese Academy of Sciences, Beijing 100029, China
[2] Graduate School of the Chinese Academy of Sciences, Beijing 100049, China
[3] Department of Mathematics, the University of Tennessee, Knoxville, TN 37996, USA
(email: zxie@lasg.iap.ac.cn, ysong@mail.iap.ac.cn, xfeng@math.utk.edu)

Abstract The seasonal change in depths of the frozen and thawed soils within their active layer is reduced to a moving boundary problem, which describes the dynamics of the total ice content using an independent mass balance equation and treats the soil frost/thaw depths as moving (sharp) interfaces governed by some Stefan-type moving boundary conditions, and hence simultaneously describes the liquid water and solid ice states as well as the positions of the frost/thaw depths in soil. An adaptive mesh method for the moving boundary problem is adopted to solve the relevant equations and to determine frost/thaw depths, water content and temperature distribution. A series of sensitivity experiments by the numerical model under the periodic sinusoidal upper boundary condition for temperature are conducted to validate the model, and to investigate the effects of the model soil thickness, ground surface temperature, annual amplitude of ground surface temperature and thermal conductivity on frost/thaw depths and soil temperature. The simulated frost/thaw depths by the model with a periodical change of the upper boundary condition have the same period as that of the upper boundary condition, which shows that it can simulate the frost/thaw depths reasonably for a periodical forcing.

Keywords: frost and thaw depth, moving boundary, Stefan problem, heat and water transfer, numerical solution

MSC(2000): 80A22

1 Introduction

The freezing-thawing processes of water in soils including change of frost/thaw depths are important components of terrestrial hydrology, which significantly influence energy and water exchanges between land surface and sub-surface, as well as vegetation growth and organic matter decomposition through thermal and hydrological processes[1]. Accurate simulation of frost and thaw depths and their climate feedback is significant for improving simulations of the hydrological and greenhouse gas exchange processes in cold regions[2]. However, current land surface models used for climate studies do not represent suitably the dynamics of frost/thaw

Received March 15, 2008; accepted May 8, 2008
DOI: 10.1007/s11425-008-0096-x
† Corresponding author
This work was supported by the National Basic Research Program (Grant No. 2005CB321703), the Knowledge Innovation Project of Chinese Academy of Sciences (Grant Nos. KZCX2-yw-126-2, KZCX2-yw-217), and the Chinese Coordinated Observation and Prediction of the Earth System project (Grant No. GYHY20070605)

depths and their feedback to the climate system, which give delayed or rapid freezing/thaw due to the frozen soil parameterization in the models[3,4]. In this paper, we try to formulate mathematically and simulate numerically the heat and water transfer processes in frozen and thawed soils. We reduce the seasonal change in depths of frozen and thawed soils to a moving boundary problem based on the first principles, which calculates frost/thaw depths based on Muller's definition[5], and then present its numerical algorithm.

To solve various moving boundary problems[6,7], some numerical methods have been developed, such as methods of lines, boundary integral, coordinate transformation, wave front tracking[8]. Crank[9] provided an introduction to the Stefan problems and presented an elaborate collection of the numerical methods used for these problems. Segal et al.[10] used an adaptive grid method in which the movement of the grid was introduced into the governing equations by the use of the total time derivative. Several implicit methods[11] have been presented for calculation and simulation of moving interface problems, such as the enthalpy method[12], VOF (Volume or Fluids) method[13,14], Level Set method[15,16] which captures the interface positions as its zero level set and the phase field method[17] based on the Kobayashi potential[17] or the Caginalp potential[18]. Due to the numerical diffusion and dispersion in the process of tracking the moving interfaces for the methods mentioned above, the contours of the moving interfaces will become vague or produce ripples.

In this paper an adaptive mesh method is presented to solve the moving boundary problem, which uses the moving interfaces as the mesh nodes to form the grid points gradually and automatically in the same fixed time step, and solves the moving interfaces and physical variables together. The moving interface at the next time step is determined according to the temperature changes at the current time step. Some numerical examinations are presented to validate the numerical model.

The remainder of this paper is organized as follows: in Section 2, we present the detailed derivation of our new mathematical model for simultaneous heat and water transfer in a one-dimensional soil column based on the first principles, and develop some explicit and implicit finite difference schemes for discrediting the governing partial differential equations (PDEs) of the proposed model; in Section 3, we do some numerical experiments with synthetic data to validate the model. We conclude the paper with a summary in Section 4.

2 A moving boundary problem for heat and water transfer processes in frozen and thawed soils and its numerical solution

In this section, we first present a detailed derivation of our one-dimensional simultaneous heat and water transfer model and then briefly describe a couple of its variants.

2.1 Governing equations of heat and water transfer in frozen and thawed soils

As shown in Figure 1, $(0, L)$ represents a one-dimensional vertical soil column with $z = 0$ denoting the land surface and $z = L$ denoting the bottom of the soil column. Phase-transition interfaces divide the soil profile into frozen and unfrozen regions, where the thermal conductive equation is satisfied. Phase changes only take place on the phase-transition interfaces[19]. Thus, the whole calculation depth is supposed to be divided into 3 layers: a thawed layer from ground surface to the first phase-transition interface (namely thaw depth), a frozen layer from the first

phase-transition interface to the second phase-transition interface (namely frost depth), and an unfrozen layer from frost depth to the bottom of calculation depth.

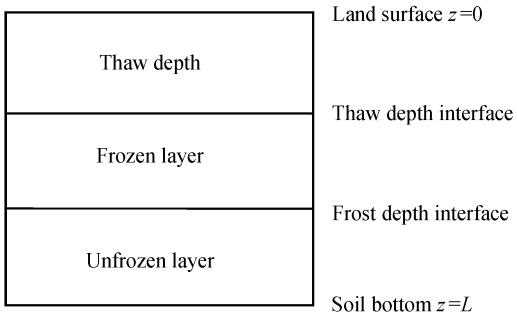

Figure 1 A schematic representation of 1-D soil column

Based on the mass and energy balance equations and temperature continuity on both phase transition interfaces, the problem can be expressed as the following equations:

$$\frac{\partial(c_u T)}{\partial t} = \frac{\partial}{\partial z}\left(\lambda_u \frac{\partial T}{\partial z}\right), \quad 0 < z < \xi,\ \varsigma < z < L, \tag{2.1}$$

$$\frac{\partial(c_f T)}{\partial t} = \frac{\partial}{\partial z}\left(\lambda_f \frac{\partial T}{\partial z}\right), \quad \xi < z < \varsigma, \tag{2.2}$$

$$\frac{\partial \theta}{\partial t} = \frac{\partial}{\partial z}\left(D\frac{\partial \theta}{\partial z}\right) - \frac{\partial K}{\partial z} + \frac{\partial q_v}{\partial z} + S, \quad 0 < z < \xi, \varsigma < z < L, \tag{2.3}$$

where t is time (s) and z is the depth of the soil column (m) (positive downwards); ξ and ς are the thaw and frost depths, respectively; c_f, c_u are volumetric soil heat capacities ($\mathrm{kJm^{-3}C^{-1}}$) of frozen and unfrozen soils, respectively; λ_f, λ_u are soil thermal conductivities ($\mathrm{Wm^{-1}C^{-1}}$) of frozen and unfrozen soils, respectively; T is soil temperature (°C); θ is the volumetric soil water content; D, K are the unsaturated soil hydraulic diffusivity ($\mathrm{m^2s^{-1}}$) and conductivity ($\mathrm{ms^{-1}}$)[20], respectively; q_v is the soil vapor flux ($\mathrm{kgm^{-2}s^{-1}}$ or $\mathrm{mms^{-1}}$)[21]; S is a sink term which represents root uptake[22−24].

To continue the derivation, we need to make some physical assumptions. The first assumption is that there is no liquid water in the frozen layer, that is, the water (and/or moisture) in the frozen layer only appears in the form of solid ice. In addition, we ignore the mechanical movement (or elastic effect) of the soil and the physical transport of the ice in the soil except at the freezing-thawing interface. Since the mechanical movement of ice is ignored, the variation of the ice content in the frozen layer is only felt through the interaction with the unfrozen zone at the freezing-thawing interface. To derive a governing equation for the ice content, our main idea is to consider the dynamics of the total ice content, instead of the ice content at each point in the frozen layer.

Let $\Delta t > 0$ be an infinitesimal time increment. When the time varies from t to $t + \Delta t$, the frozen zone changes from $(\xi(t), \varsigma(t))$ to $(\xi(t + \Delta t), \varsigma(t + \Delta t))$, and then the change of the total ice mass in the frozen zone over the time period $[t, t + \Delta t]$ is

$$\int_{\xi(t+\Delta t)}^{\varsigma(t+\Delta t)} \theta_i(z, t + \Delta t)\rho_i dz - \int_{\xi(t)}^{\varsigma(t)} \theta_i(z, t)\rho_i dz, \tag{2.4}$$

where θ_i denotes the ice content, ρ_i is the density of the ice.

On the other hand, the total ice mass change due to boundary movement over the time interval $[t, t+\Delta t]$ can also be computed approximately by

$$\rho_i(t)\theta_i(\xi,t)(\xi(t+\Delta t)-\xi(t))+\rho_i(t)\theta_i(\varsigma,t)(\varsigma(t+\Delta t)-\varsigma(t)). \tag{2.5}$$

Equating the expressions in (2.4) and (2.5) yields

$$\begin{aligned}\int_{\xi(t+\Delta t)}^{\varsigma(t+\Delta t)}\theta_i(z,t+\Delta t)\rho_i dz-\int_{\xi(t)}^{\varsigma(t)}\theta_i(z,t)\rho_i dz\\ \approx \rho_i(t)\theta_i(\xi,t)(\xi(t+\Delta t)-\xi(t))+\rho_i(t)\theta_i(\varsigma,t)(\varsigma(t+\Delta t)-\varsigma(t)).\end{aligned} \tag{2.6}$$

Dividing the both sides by Δt, and taking the limit $\Delta t\to 0$, we get

$$\frac{d}{dt}\int_{\xi(t)}^{\varsigma(t)}\theta_i\rho_i dz=\left(\rho_i\theta_i\frac{d\xi}{dt}\right)\Big|_{z=\xi(t)}+\left(\rho_i\theta_i\frac{d\varsigma}{dt}\right)\Big|_{z=\varsigma(t)}. \tag{2.7}$$

The moving boundary conditions can be described as follows:

$$T|_{z=\xi^+}=T|_{z=\xi^-}=T_f,\quad T|_{z=\varsigma^+}=T|_{z=\varsigma^-}=T_f, \tag{2.8}$$

$$Q\frac{d\xi}{dt}=\lambda_f\frac{\partial T}{\partial z}\Big|_{z=\xi}-\lambda_u\frac{\partial T}{\partial z}\Big|_{z=\xi},\quad Q\frac{d\varsigma}{dt}=\lambda_f\frac{\partial T}{\partial z}\Big|_{z=\varsigma}-\lambda_u\frac{\partial T}{\partial z}\Big|_{z=\varsigma}, \tag{2.9}$$

$$\frac{d\xi}{dt}=q_l(\xi,t),\quad \frac{d\varsigma}{dt}=q_l(\varsigma,t), \tag{2.10}$$

where T_f is freezing temperature (°C); Q is heat released by unit volume of soil during the freezing process (kJm^{-3}), which can be expressed as follows:

$$Q=L_f\gamma_d(W-W_u), \tag{2.11}$$

where L_f is latent heat (334.5kJ/kg), γ_d is dry density (kg/m^3), W is water content of soil (%), and W_u is unfrozen water content of soil (%).

Equations (2.8), (2.9) and (2.10) describe the temperature continuity, the energy balance on both phase-transition interfaces, and mass balance on the interfaces, respectively.

The initial and boundary conditions for the moving boundary problem are as follows:

$$T(z,0)=g_1(z), 0<z<L,\quad \theta(z,0)=g_2(z),\quad 0<z<L, \tag{2.12}$$

$$T(0,t)=f_1(t),\quad t>0,\quad q_l(0,t)=f_2(t),\quad t>0, \tag{2.13}$$

$$\frac{\partial T}{\partial z}|_{z=L}=G_g,\quad \theta(L,t)=\theta_r,\quad t>0, \tag{2.14}$$

where $f_1(t), f_2(t)$ are soil surface temperature (°C) and infiltration, respectively; $g_1(t), g_2(t)$ are soil initial temperature (°C) and volumetric water content, respectively; G_g is soil bottom heat flux (°C/m); θ_r is residual water content; and q_l is flow flux (m/s).

Remark 1. The above model can be used as module to build composite models that describe multi-layered freezing and/or thawing processes. Such a model, which involves multiple moving interfaces, can be utilized to describe a complicated freezing and thawing process in a seasonal frozen soil.

Remark 2. The above one-dimensional model can be easily generalized to higher dimensions with help of the Gibbs-Thompson condition[25] to describe the surface tension on the interface.

2.2 Finite difference approximations and computation algorithm

Since the mathematical model developed in the previous section is highly nonlinear and involves two unknown moving interfaces/boundaries, it is not possible to find closed form analytical solutions for the model. Consequently, the only feasible way to solve the problem is to compute approximate numerical solutions. We shall first construct some explicit and implicit finite difference methods for approximating the one-dimensional model, and then present a computation algorithm for implementing the proposed finite difference schemes on computers.

First, we need some notations. Let $\{t_k\}_{k\geqslant 0}$ be a sequence of equally spaced time points with the time step Δt. Let $\mathcal{T}_h := \{z_j;\, j = 1, 2, \ldots, J\}$ be a mesh for the interval $[0, L]$ with $z_1 = 0$ and $z_J = L$. Let ξ^k denote an approximation to $\xi(t_k)$, ς^k denote an approximation to $\varsigma(t_k)$, define $\mathcal{T}_h^0 := \mathcal{T}_h \cup \{\xi^0, \varsigma^0\}$ and $\mathcal{T}_h^k := \mathcal{T}_h \cup \{\xi^k, \varsigma^k\}$ for $k \geqslant 1$, that is, $\mathcal{T}_h^k$ contains all the mesh points of $\mathcal{T}_h$ and the two computed interface points. Set $h_j := z_j - z_{j+1}$ and $h_{j+\frac{1}{2}} := \frac{1}{2}(h_{j+1} + h_j)$ for $j = 1, 2, \ldots, J_k - 1$, where J_k denotes the total number of nodes in the mesh $\mathcal{T}_h^k$. Note that the number of distinct nodes in $[0, L]$ is at most $J+2$ at each time step t_k for $k \geqslant 0$, i.e., $J \leqslant J_k \leqslant J + 2$. It is possible to choose $\mathcal{T}_h^{k+1}$ completely different from and independent of $\mathcal{T}_h^k$ as long as $\{\xi^{k+1}, \varsigma^{k+1}\} \in \mathcal{T}_h^{k+1}$. Such a technique is known as an adaptive mesh method[26].

For a given sequence of numbers $\{\eta_j^k\}$, we define the following difference operators:

$$D^b\eta_j^k := \frac{\eta_j^k - \eta_j^{k-1}}{\Delta t}, \quad E_f\eta_j^k := \frac{\eta_{j+1}^k - \eta_j^k}{h_{j+1}}, \quad E_b\eta_j^k := \frac{\eta_j^k - \eta_{j-1}^k}{h_j}, \quad E_c\eta_j^k := \frac{\eta_{j+1}^k - \eta_{j-1}^k}{h_j + h_{j+1}}.$$

Now, we are ready to discretize equations (2.1)–(2.3). The general guidelines we follow here are to use a backward difference for temporal discretization and to use a central difference for spatial discretization. As a result, we obtain a family of implicit finite difference schemes (including an explicit scheme) with a truncation error of order $O(\Delta t + h^2)$, where $h = \max\{h_j; j = 1, 2, \ldots, J_k\}$. Hence, our finite difference approximations for equations (2.1)–(2.3) are defined as follows:

$$\begin{aligned} D^b\theta_j^{k+1} &- \frac{\omega}{h_{j+\frac{1}{2}}}(D_{j+\frac{1}{2}}^{k+1}E_f\theta_j^{k+1} - D_{j-\frac{1}{2}}^{k+1}E_b\theta_j^{k+1}) \\ &- \frac{(1-\omega)}{h_{j+\frac{1}{2}}}(D_{j+\frac{1}{2}}^{k}E_f\theta_j^{k} - D_{j-\frac{1}{2}}^{k}E_b\theta_j^{k}) - \omega E_cK_j^{k+1} - (1-\omega)E_cK_j^k - S_j \\ &- \omega\frac{q_{vj+1}^{k+1} - q_{vj-1}^{k+1}}{h_j + h_{j+1}} - (1-\omega)\frac{q_{vj+1}^{k} - q_{vj-1}^{k}}{h_j + h_{j+1}} = 0, \end{aligned} \tag{2.15}$$

$$\begin{aligned} D^b(c_{uj}^{k+1}T_j^{k+1}) &- \frac{\omega}{h_{j+\frac{1}{2}}}(\lambda_{uj+\frac{1}{2}}^{k+1}E_fT_j^{k+1} - \lambda_{uj-\frac{1}{2}}^{k+1}E_bT_j^{k+1}) \\ &- \frac{(1-\omega)}{h_{j+\frac{1}{2}}}(\lambda_{uj+\frac{1}{2}}^{k}E_fT_j^{k} - \lambda_{uj-\frac{1}{2}}^{k}E_bT_j^{k}) = 0, \end{aligned} \tag{2.16}$$

for $j = 1, 2, \ldots, j_{k1} - 1$ or $j = j_{k2} + 1, \ldots, J_k - 1$ and $0 \leqslant \omega \leqslant 1$, and

$$\begin{aligned} D^b(c_{fj}^{k+1}T_j^{k+1}) &- \frac{\omega}{h_{j+\frac{1}{2}}}(\lambda_{fj+\frac{1}{2}}^{k+1}E_fT_j^{k+1} - \lambda_{fj-\frac{1}{2}}^{k+1}E_bT_j^{k+1}) \\ &- \frac{(1-\omega)}{h_{j+\frac{1}{2}}}(\lambda_{fj+\frac{1}{2}}^{k}E_fT_j^{k} - \lambda_{fj-\frac{1}{2}}^{k}E_bT_j^{k}) = 0, \end{aligned} \tag{2.17}$$

for $j = j_{k_1}, \ldots, j = j_{k_2}$ and $0 \leqslant \omega \leqslant 1$. Clearly, when the relaxation parameter $0 \leqslant \omega \leqslant 1$, the above scheme is implicit, in particular, $\omega = 1$ and $\omega = 0$ give the backward Euler scheme and the explicit Euler scheme, respectively.

Next, we update the interface point by equation (2.9) as follows:

$$Q^k D^b \xi^{k+1} = \left(\lambda_f \frac{\partial T}{\partial z}\bigg|_{z=\xi^k} - \lambda_u \frac{\partial T}{\partial z}\bigg|_{z=\xi^k} \right)_{j_{k1}}, \tag{2.18}$$

$$Q^k D^b \varsigma^{k+1} = \left(\lambda_f \frac{\partial T}{\partial z}\bigg|_{z=\varsigma^k} - \lambda_u \frac{\partial T}{\partial z}\bigg|_{z=\varsigma^k} \right)_{j_{k2}}. \tag{2.19}$$

Finally, interface condition (2.10) can be discretized by any 3-point (not 2-point) difference approximation to maintain an overall truncation error of order $O(\Delta t + h^2)$.

To implement the above finite difference methods on computers, we propose the following computation algorithm.

Algorithm

Step 1. Choose the initial datum functions $g_1(z), g_2(z), \xi^0, \varsigma^0$. Set $z_{j_{k1}} = \xi^0, z_{j_{k2}} = \varsigma^0$ and k: $= 0$.

Step 2. Compute $\theta_j^{k+1}, T_j^{k+1}, \xi^{k+1}, \varsigma^{k+1}$ by solving the nonlinear algebraic system (2.15)–(2.19) using an iterative nonlinear solver (e.g. Newton's method).

Step 3. Check whether the stopping criterion is met. If the relative error of two iterates is less than a prescribed tolerance, stop the iteration and set $k := k + 1$, go back to Step 2. Otherwise, let the iteration run until the maximum number of iterations is reached, then either stop or set $k := k + 1$ and go back to Step 2. Continue the time integration until $t_{k+1} = t_{\text{final}}$.

3 Numerical simulations

Based on the equations (2.1)–(2.3), (2.7)–(2.10) and (2.12)–(2.14) together with the finite difference algorithms (2.15)–(2.19), we develop a numerical model, which combines the one-dimensional heat and water transfer model and the numerical algorithm described in Section 2. To validate the numerical model, we take in this section the upper boundary condition for temperature as the following function:

$$f_1(t) = T_0 + G_t t + A\sin(\omega t), \tag{3.1}$$

where $T_0 = 0$ is mean annual ground surface temperature (GST) (°C); $G_t = 0.02$ is the rising rate of GST ($^\circ\mathrm{C} \cdot \mathrm{a}^{-1}$); $A = 13^\circ$C is annual amplitude of GST, i.e., half of annual GST differences; $\omega = \frac{2\pi}{8760}$. The zero infiltration boundary at the land surface is used. The zero heat-flux boundary condition and residual water content $\theta_r = 0.05$ at the bottom of the soil column are used. We set initial temperature as $g_1(z) = 1 - \frac{z}{L}$, and initial water content as $g_2(z) = 0.06$. Thermal conductivities in the frozen and thawed soils are set as $1.57\mathrm{Wm}^{-1}\mathrm{K}^{-1}$ and $1.28\mathrm{Wm}^{-1}\mathrm{K}^{-1}$, respectively, volumetric heat capacities in the frozen and thawed soils are $1872\mathrm{Jm}^{-3}\mathrm{K}^{-1}$ and $2475\mathrm{Jm}^{-3}\mathrm{K}^{-1}$ [19], respectively, saturated hydraulic conductivity $K_s = 1.2e-4\mathrm{m/s}$, and $b = 4.2$ [27].

Several sensitivity experiments were performed to evaluate the model. They include (1) Run 1, using the parameters set above with $L = 30$ m; (2) Run 2, using the parameters set above

with different soil depths $L = 3\text{m}, 30\text{m}, 100\text{m}$; (3) Run 3, the parameters set above with different T_0; (4) Run 4, the parameters set above with different A; (5) Run 5, the parameters set above with different thermal conductivities. The detail values are listed in Table 1.

Table 1 Parameters set for sensitivity experiments

	Run 1	Run 2	Run 3	Run 4	Run 5
L (m)	30	3,30,100	30	30	30
T_0 (°C)	0	0	1,0,−1,−2	0	0
A (°C)	13	13	13	$1, 2, 5$	13
Factor	1	1	1	1	$1, 0.25, 0.5, 1.5$

The upper boundary condition of surface temperature and the simulated frost and thaw depths are shown in Figure 2. We can see that the simulated frost and thaw depths have a periodic change which fits well with that of the soil surface temperature. The phase difference between the period of the temperature and that of frost depth is 2 days, and the phase difference between that of the surface temperature and that of the thaw depth is 11 days. Furthermore, with the rising rate of GST $G_t = 0.02$°C/a, the soil surface temperature keeps increasing. Accordingly, the minimum of frost depth and maximum of thaw depth become deeper.

To consider the effect of the soil depth in the model on the simulated frost and thaw depths, and soil temperature, we do the simulations by the numerical model with the initial and boundary conditions mentioned above for the soil depths L= 3m, 30m, and 100m. Figure 3(a) shows

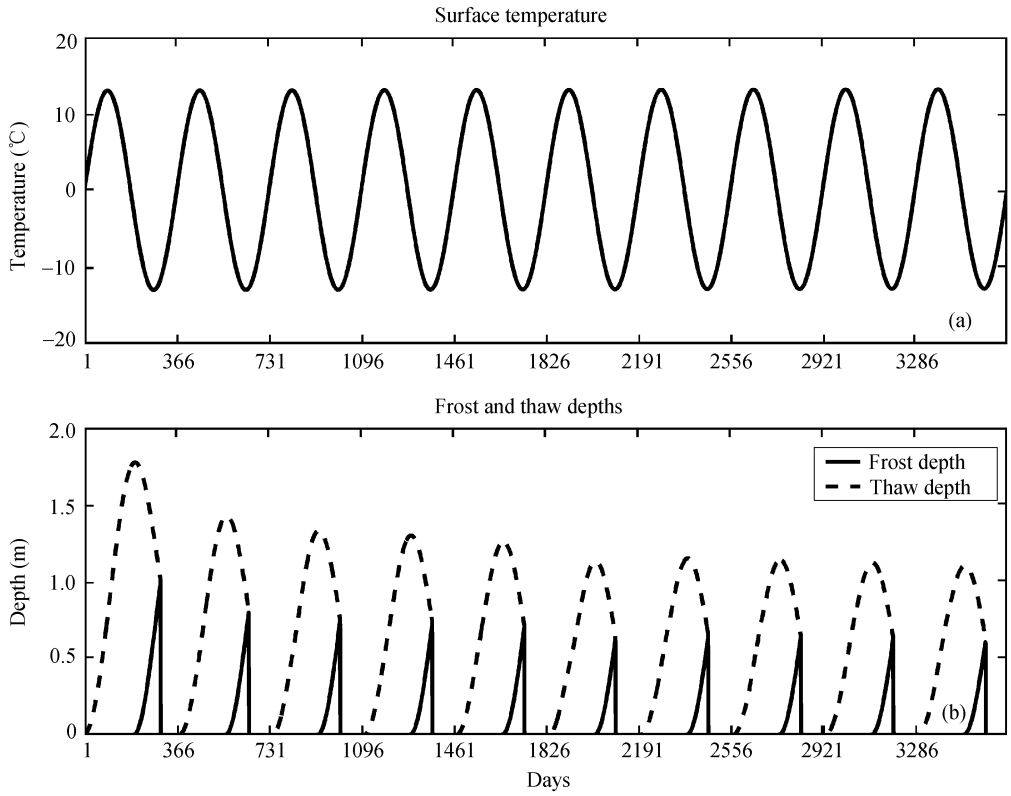

Figure 2 (a) soil surface temperature, (b) simulated frost and thaw depths

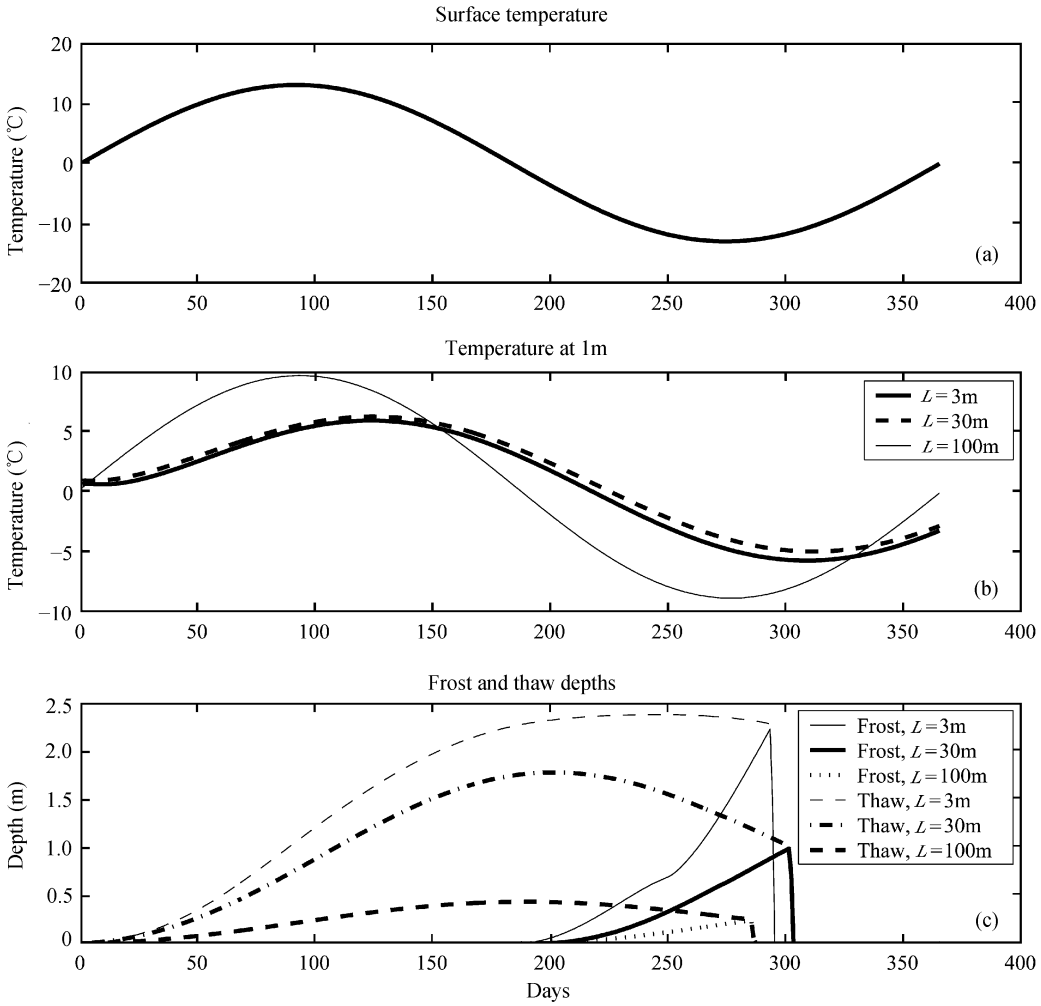

Figure 3 Sensitivities to the soil depth. (a) Surface temperature, (b) temperature at 1m, (c) frost and thaw depths

the soil surface temperature. The simulated soil temperatures at 1m for $L = 3\text{m}, 30\text{m}, 100\text{m}$ are shown in Figure 3(b). We can see that the simulated temperature for $L = 3\text{m}$ is closer to that for $L = 30\text{m}$, the difference between the two cases is from $-1°\text{C}$ to $0°\text{C}$; the model with $L = 100\text{m}$ overshoots and undershoots the simulated soil temperature compared with cases for $L = 3\text{m}$ and 30m. The difference can be as big as $4 - 10°\text{C}$ on timescale of one year. The simulated cooling and warming at 1 m by the model with $L = 100\text{m}$ are advanced by approximately 30 days than the cases for $L = 3\text{m}$, and $L = 30\text{m}$.

The simulated frost and thaw depths are shown in Figure 3(c). The periods of the freezing-thawing process are about 295 days, 303 days and 297 days for the three soil depths L= 3m, 30m, and 100m, respectively. For the three simulated cases, soil begins to freeze on about the 200th day, and reach its maximum thaw depth at the 200th day. The simulated depths for L=100m do not exceed 0.5m, and which are underestimated than those for L=3m and L=30m, which reach the maximum depth about 2m. It is maybe that the same space step compartmentalize method is coarser to the soil depth L= 100m, and leads to the imprecise results.

Next we fix the simulated soil depth ($L = 30$m). Four values of mean surface temperature, i.e., $T_0 = 1, 0, -1$ and -2°C, are input into the model. Figure 4(a) shows the simulated soil temperatures for $T_0 = 1, 0, -1$ and -2°C at 1m. We can see that the periodic change of the simulated temperatures at 1m fits well that of the surface temperature on the timescale. The maximum soil temperature and the minimum temperature for the four cases are reached at about the 124th day and the 311th day, respectively. With warmer T_0, the simulated soil temperature gets higher. The differences among the simulated temperatures for the four cases are between about -1°C and 2°C.

Figure 4(b) shows the simulated frost and thaw depths under the four conditions. We can see that when T_0 is warmer, the amplitudes of thaw depth change larger and the amplitudes of frost depth change less, especially when $T_0 > 0$. This indicates that frost and thaw depths are related with the mean surface temperature nearly.

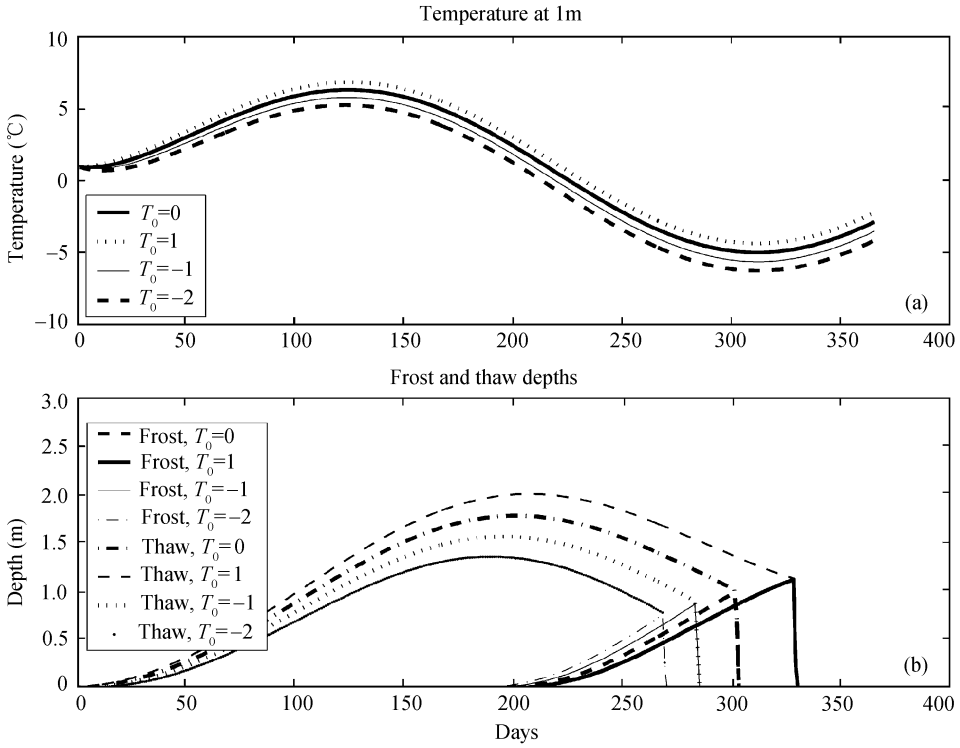

Figure 4 Sensitivity to T_0($T_0 = 1, 0, -1$ and -2°C). (a) For temperature at 1m, (b) for frost and thaw depths

Figure 5(a) shows the simulated soil temperatures at 1m for $A = 1, 2, 5$°C. The amplitude for the simulated soil temperature with $A = 5$°C is largest, and it decreases with decreased A. The difference is between -2°C and 1.5°C.

Figure 5(b) shows the simulated frost and thaw depths by the numerical with $T_0 = 0$, and the annual amplitude of GST $A = 1, 2$, and 5°C. Under the three conditions, soil begins to freeze and thaw depths reach its maximum on the $200th$ day. The simulated depths get deeper gradually with the annual amplitude of GST increased, and the maximum difference of the simulated maximum depths is about 0.6m.

Finally, a sensitivity experiment by the model to the thermal conductivity with $A = 13$°C,

$T_0 = 0°C$ is presented. Figure 6(a) shows the simulated soil temperatures at 1m using thermal conductivity with the factors 0.25, 0.5, 1 and 1.5. We can see that the temperatures become

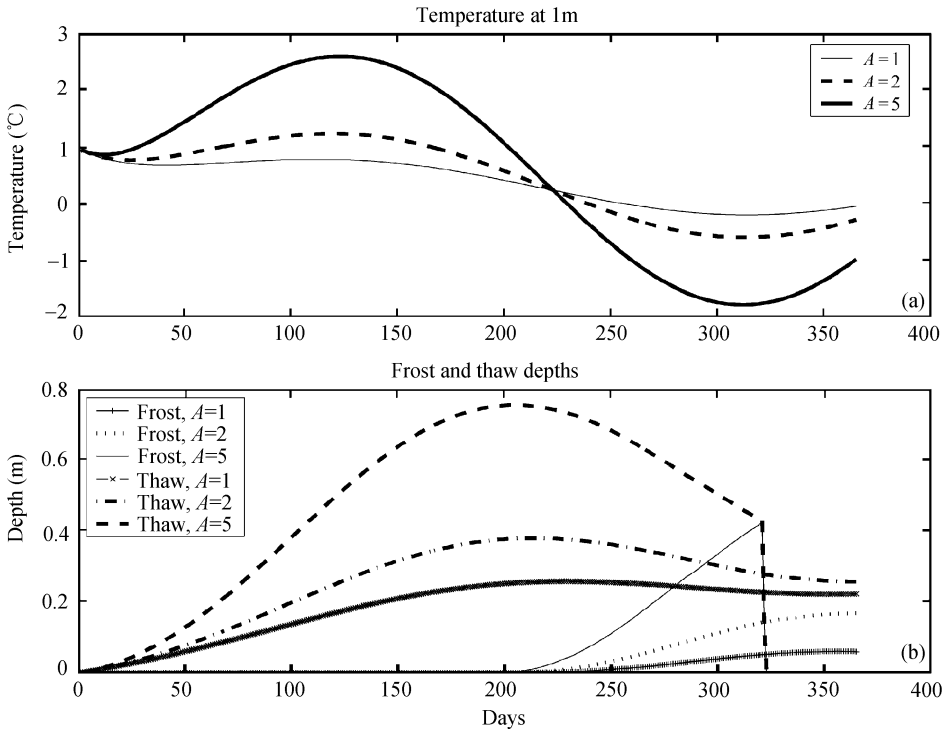

Figure 5 Sensitivity to A: (a) For temperature at 1m, (b) for frost and thaw depths

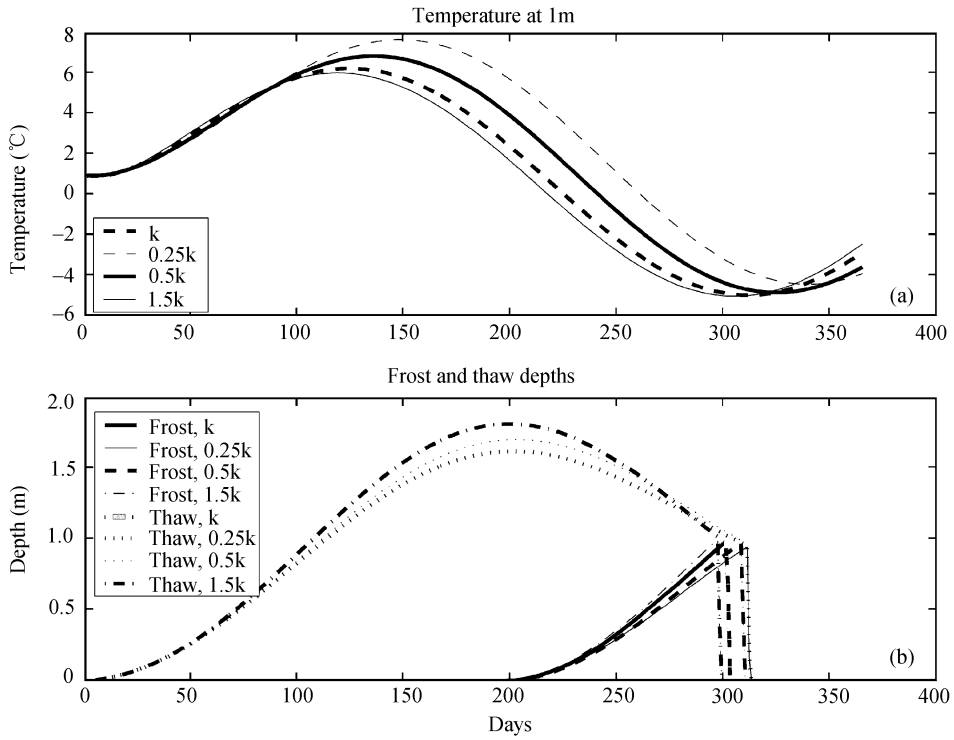

Figure 6 Sensitivity to the soil thermal conductivity. (a) For temperature at 1m, (b) for frost and thaw depths

low with increased thermal conductivity, which fits with the property of the thermal conductivity. When thermal conductivity is larger, the heat flux through the soil becomes larger, and hence the soil temperature is lower.

Figure 6(b) shows the simulated frost and thaw depths using thermal conductivity with the factors 0.25, 0.5, 1 and 1.5. The simulated thaw and frost depths and the length of the period for difference factors show some differences. The simulated depths reach their maximum values at thermal conductivity with the factor 1.5 and minimum values with factor 0.25. The difference of frost depths for the factors mentioned above and that of thaw depths for the factors are about 0.2m, respectively. It indicates that difference for the different thermal conductivities is not large.

4 Summary and concluding remarks

This paper develops a new simultaneous heat and water transfer model for simulating the active layer and frost/thaw depth in frozen and thawed soil. Mathematically, the model is described by a set of nonlinear partial differential equations coupled with a moving interface/boundary. Unlike the existing models, the new model explicitly tracks the freezing-thawing interface and frost/thaw depths, and uses an independent mass balance equation to describe the dynamics of the total ice content in the model. Numerical simulations are presented to validate the proposed numerical model and to investigate the effects of the thickness of the soil, ground surface temperature, amplitude of ground surface temperature and thermal conductivity on frost/thaw depths and soil temperature. From above studies, it is found that design parameters affect frost/thaw depth and soil temperature differently. The thickness of the soil and thermal conductivity have the important influence on frost/thaw depth and soil temperature. Furthermore, the periodic variety of frost/thaw depth fits well with that of the upper boundary condition.

Acknowledgements The third author gratefully acknowledges the support of K. C. Wong Education Foundation, Hong Kong.

References

1 Woo M K, Winter T C. The role of permafrost and seasonal frost in the hydrology of northern wetlands in North America. *J Hydrol*, **141**: 5–31 (1993)
2 Luo L, Robock A, Vinnikov K Y, et al. Effects of frozen soil on soil temperature, spring infiltration and runoff: Results from the PILPS 2 (d) experiment at Valdai, Russia. *J Hydrometeorology*, **4**: 334–351 (2003)
3 Niu G Y, Yang Z L. Effects of frozen soil on snowmelt runoff and soil water storage at a continental scale. *J Hydrometeorology*, **7**: 937–952 (2006)
4 Cogley J G, Pitman A J, Henderson-Sellers A. A land surface for large-scale climate models. Tech Note 90-1. Peterborough, Ont: Trent Univ, 1990
5 Muller S W. Permafrost or Permanently Frozen Ground and Related Engineering Problems. Ann Arbor, Mich: Edwards, 1947
6 Javierre E, Vuik C, Vermolen F J, Zwaag S van der. A comparison of numerical models for one-dimensional Stefan problems. *J Comput Appl Math*, **192**: 445–459 (2006)
7 Liu Q, Shui H S, Zhang X Y. Advances in numerical simulation of interfacial/free-surfaces flows (in Chinese). *Adv Mech*, **32**(2): 259–274 (2002)
8 Wang Z F, Liu R X. Front tracing methods (in Chinese). *Mechanics and Practice*, **22**: 1–14 (2000)
9 Crank J Free and Moving Boundary Problems. Oxford: Clarendon Press, 1984
10 Segal G, Vuik C, Vermolen F. A conserving discretization for the free boundary in a two-dimensional Stefan problem. *J Compute Phys*, **141**: 1–21 (1998)

11 Liu R X, Wang Z F. Methods of Numerical Simulation and Tracking for Moving Interfaces (in Chinese). Hefei: University of Science and Technology of China Press, 2001
12 Minkowycz W J, Sparrow E M. Advances in Numerical Heat Transfer **1**. Washington: Taylor & Francis, 1997
13 Hirt C W, Nichols B D. Volume of fluid (VOF) method for the dynamics of free boundaries. *J Comput Phys*, **39**: 201–225 (1981)
14 Gueyfier D, Li J. Volume-of-fluid interface tracking with smoothed surface stress methods for 3D flows. *J Comput Phys*, **152**(2): 423–456 (1999)
15 Osher S, Sethian J A. Fronts propagating with curvature-dependent speed: algorithms based on Hamilton-Jacobi formulations. *J Comput Phys*, **79**: 12–49 (1988)
16 Vermolen F J, Javierre E, Vuik C, Zha L, Zwaag S van der. A three-dimensional model for particle dissolution in binary alloys. *Comput Materials Science*, **39**: 767–774 (2007)
17 Wheeler A A, Boettinger W J, McFadden G B. Phase field model for isothermal phase transitions in binary alloys. *Phys Rev A*, **45**: 7424–7439 (1992)
18 Mackenzie J A, Robertson M L. A moving mesh method for the solution of the one-dimensional phase field equations. *J Comput Phys*, **181**: 526–544 (2002)
19 Nan Z T, Li S X, Cheng G D. Prediction of permafrost distribution on the Qinghai-Tibet Plateau in the next 50 and 100 years. *Sci China Ser D-Earth Sci*, **48**(6): 797–804 (2005)
20 Clapp R B, Hornberger G M. Empirical equations for some soil hydraulic properties. *Water Resource Res*, **14**: 601–604 (1978)
21 Sun S F. Parameterization Study of Physical and Biochemical Mechanism in Land Surface Process (in Chinese). Beijing: China Meteorology Press, 2005
22 Gardner W R. Relation of root distribution to water uptake and availability. *Agron J*, **56**: 35–41 (1964)
23 Molz F J, Remson I. Extraction term models of soil moisture use by transpiring plants. *Water Resource Res*, **6**: 1346–1356 (1970)
24 Lei Z D, Yang S X, Xie S H. Soil Water Dynamics (in Chinese). Beijing: Tsinghua University Press, 1998
25 Visintin. Models of phase transitions. Progress in Nonlinear Differential Equations and Their Applications. Boston: Birkhäuser, 1996
26 Bangerth W, Rannacher R. Adaptive Finite Element Methods for Differential Equations. New York: Birkhäuser, 2003
27 Li X, Koike T. Frozen soil parameterization in SiB2 and its validation with GAME -Tibet observations. *Cold Regions Science and Technology*, **36**(1–3): 165–182 (2003)